Environ. Eng. Res. 2018; 23(3): 339-344
https://doi.org/10.4491/eer.2018.041

pISSN 1226-1025
eISSN 2005-968X

# An important factor for the water gas shift reaction activity of Cu-loaded cubic $Ce_{0.8}Zr_{0.2}O_2$ catalysts

**Won-Jun Jang[1], Hyun-Seog Roh[1†], Dae-Woon Jeong[2†]**

[1]*Department of Environmental Engineering, Yonsei University, Wonju 26493, Republic of Korea*
[2]*School of Civil, Environmental and Chemical Engineering, Changwon National University, Changwon 51140, Republic of Korea*

**ABSTRACT**

The Cu loading of a cubic $Ce_{0.8}Zr_{0.2}O_2$-supported Cu catalyst was optimized for a single-stage water gas shift (WGS) reaction. The catalyst was prepared by a co-precipitation method, and the WGS reaction was performed at a gas hourly space velocity of 150,494 $h^{-1}$. The results revealed that an 80 wt% Cu-$Ce_{0.8}Zr_{0.2}O_2$ catalyst exhibits excellent catalytic performance and 100% $CO_2$ selectivity ($X_{CO}$ = 27% at 240°C for 100 h). The high activity of 80 wt% Cu-$Ce_{0.8}Zr_{0.2}O_2$ catalyst is attributed to the presence of abundant surface Cu atoms and the low activation energy of the resultant process.

**Keywords:** Activation energy, $Ce_{0.8}Zr_{0.2}O_2$, Cu atoms, Cu loading

## 1. Introduction

Modern fuel cells, which are widely used in portable electronic devices and for mobile energy generation, are significantly more efficient than the current internal combustion engines and are environmentally friendly, producing no $CO_x$, $NO_x$, hydrocarbons, or soot [1]. The water gas shift (WGS) reaction plays an important role in such technologies. This reaction is reversible and exothermic, as shown below [2]:

$$CO + H_2O \leftrightarrow CO_2 + H_2,\ \Delta H = -40.6\ kJ\ mol^{-1} \quad (1)$$

At the industrial level, the WGS reaction is performed in two steps to overcome thermodynamic limitations. The first step is a high temperature shift (HTS, 350℃ - 450℃) reaction, typically performed over $Fe_2O_3/Cr_2O_3$ catalysts, and the second is a low temperature shift (LTS, 180℃ - 250℃) reaction, typically performed over $Cu/Zn/Al_2O_3$ catalysts [3]. The HTS reaction is more critical compared with the LTS reaction for compact fuel processors that feature integrated on-board hydrogen production because the first-step reactor typically occupies ca. 70% of the total volume of such systems. Consequently, a robust single-stage WGS reactor is desirable for compact fuel cell systems [4]. However, commercial WGS catalysts are not suitable for compact reformers owing to restrictions in volume, weight, and cost [5]. Furthermore, commercial WGS catalysts are pyrophoric and require complex preconditioning steps [5]. As a result, precious-metal-based catalysts have been explored in an attempt to overcome these limitations.

Precious metals, such as Pt, Pd, and Au, supported on reducible oxides ($CeO_2$, $TiO_2$, and $Fe_2O_3$) have been reported as promising next-generation catalysts that exhibit excellent performance in the WGS reaction at low temperatures [6-9]. However, the high cost and scarcity of these metals inhibit their utility for industrial-scale applications. Thus, the design and synthesis of cost-effective precious-metal-free catalysts for single-stage WGS reaction in compact reformers are highly desirable.

In our previous study, we investigated the Ce/Zr ratio in Cu-$CeO_2$-$ZrO_2$ catalysts employed in the LTS step [10]. A cubic-phase Cu-$Ce_{0.8}Zr_{0.2}O_2$ catalyst exhibited the highest turnover frequency and lowest activation energy of the catalysts tested, and its CO conversion was maintained for 100 h. The excellent performance of this catalyst was attributed to the presence of abundant oxygen vacancies and the strong interaction between CuO and cubic-phase $Ce_{0.8}Zr_{0.2}O_2$.

Although the $CeO_2$-$ZrO_2$ support with high oxygen vacancy was found to play an important role in enhancing activity, but the behavior of Cu active species is not completely understood.



**Received** January 22, 2018 **Accepted** March 21, 2018

† Corresponding author
Email: hsroh@yonsei.ac.kr, dwjeong@changwon.ac.kr
Tel: +82-55-213-3743 Fax: +82-55-281-3011
ORCID: 0000-0002-5064-2314 (H-S Roh) / 0000-0003-1842-3047 (D-W Jeong)

Typically, the amount of Cu active species can be controlled by varying the loading amount of Cu. However, the characteristics of Cu species appear to be strongly influenced by the Cu sintering [11]. Therefore, a further investigation into the effect of Cu loading on the physicochemical property and catalytic performance of Cu-$Ce_{0.8}Zr_{0.2}O_2$ catalysts is necessary. In particular, the correlation of the characteristic of Cu species with turnover frequency & CO conversion is elucidated.

Consequently, in the present study, we focused on optimizing the Cu loading in a cubic $Ce_{0.8}Zr_{0.2}O_2$-supported Cu catalyst to further improve its performance. For this approach, we synthesized a series of catalysts with different Cu loadings in the range of 20 wt% - 90 wt% and evaluated their LTS-reaction performances in the temperature range of 240℃ - 320℃. Furthermore, the catalysts were characterized by Brunauer-Emmett-Teller (BET) surface area analysis, X-ray diffraction (XRD), $N_2O$-chemisorption, and temperature-programmed reduction (TPR), and the results of these analyses were discussed in terms of the WGS reaction activity.

## 2. Experimental

### 2.1. Catalyst Preparation

Cu-$Ce_{0.8}Zr_{0.2}O_2$ catalysts with various Cu loading amounts (20, 40, 60, 80, and 90 wt%) were synthesized using a one-step co-precipitation method. First, appropriate stoichiometric quantities of $Cu(NO_3)_3{\cdot}xH_2O$ (99%, Aldrich), $Ce(NO_3)_3{\cdot}6H_2O$ (99%, Aldrich) and zirconyl nitrate solution (20 wt% $ZrO_2$ basis, MEL Chemicals) were dissolved in distilled water. Then, 15 wt% KOH solution was added dropwise at 80℃ with constant stirring to attain pH 10.5. The resultant precipitate was aged at 80℃ for 3 d. The obtained materials were washed, collected, and air-dried for 24 h and then dried at 110℃ for 6 h. The dried materials were crushed into powder and annealed in a furnace at 400℃ for 6 h. These final products were used in the WGS reaction.

### 2.2. Characterization

The BET surface areas of the catalysts were measured using a nitrogen physisorption technique on an ASAP 2010 (Micromeritics) accelerated surface area and porosimetry instrument. Before analysis, the samples were degassed for 12 h at 110℃ under a pressure of less than 0.5 mm Hg. XRD was performed using a Rigaku D/MAX-IIIC diffractometer operated at 40 kV and 100 mA with Ni-filtered CuKα radiation. The crystallite size was calculated from the diffraction pattern using the Scherrer equation.

$$D = \frac{K\lambda}{\beta \cos\theta} \tag{2}$$

where $D$ is the crystallite size, $K$ is the shape factor (0.89 for a sphere), $\lambda$ is the wavelength of Cu $K_a$ (1.54 Å), $\beta$ is the full width half maximum (FWHM), and $\theta$ is the Bragg diffraction angle. TPR experiments were performed using an Autochem 2910 (Micromeritics) instrument. The TPR experiments were conducted as described in previous papers [12, 13]. The $N_2O$-chemisorption experiments were performed using an Autochem 2920 (Micromeritics) instrument. Before $N_2O$-chemisorption, the fresh samples were reduced at 250℃ for 2 h in 10 vol% $H_2$/Ar. The consumption of $N_2O$ and release of $N_2$ by the metallic Cu sites at 60℃ ($N_2O + 2Cu \rightarrow Cu_2O + N_2$) were monitored using a thermal conductivity detector.

### 2.3. Catalytic Reaction

Activity tests were conducted by the same quartz reactor used in our previous study [10]. Before starting the reaction, the catalyst was reduced at 400℃ for 1 h under a stream of 5% $H_2/N_2$. The catalyst was then evaluated at different reaction temperatures covering the range of 200℃ - 400℃. A gas hourly space velocity (GHSV) of 72,152 $h^{-1}$ was employed to screen the catalysts in this study. A mass flow controller (Brooks Instrument 5850E) was used to feed the gaseous mixture (6.5 vol% CO, 7.1 vol% $CO_2$, 0.7 vol% $CH_4$, 42.4 vol% $H_2$, 28.7 vol% $H_2O$, and 14.5 vol% $N_2$), and a syringe pump was installed to supply water. A heating coil for vaporizing water was wrapped around the gas feed line close to the quartz reactor. The product gas from the reactor was monitored by an online micro-gas chromatographer (Agilent 3000) equipped with a molecular sieve and PLOT U columns.

The turnover frequency (TOF) was measured in separate experiments wherein the conversion of CO was kept below 20% so that the differential reaction conditions could be assumed with negligible heat and mass-transfer effects. TOF was calculated using the equation:

$$TOF = \frac{(CO_{in} - CO_{out})AB_M F}{DWX_M} \tag{3}$$

where $CO_{in}$ and $CO_{out}$ are the inlet and outlet concentrations of CO, respectively, $AB_M$ is the atomic weight of metal M, $F$ is the total flow rate (mol $s^{-1}$), $D$ is the metal dispersion, $W$ is the mass of catalyst (g), and $X_M$ is the metal content ($g_{metal}$ $g_{cat}^{-1}$).

The Arrhenius plot can be obtained from the relationship between TOF and temperature.

$$\ln TOF = -\frac{E_a}{R}\left(\frac{1}{T}\right) + \ln A \tag{4}$$

where $A$ is the pre-exponential factor, $T$ is the reaction temperature (K), $R$ is the ideal gas constant (J/mol·K), and $E_a$ is the activation energy (kJ/mol).

## 3. Results and Discussion

### 3.1. Catalyst Characterization

The XRD patterns of the Cu-$Ce_{0.8}Zr_{0.2}O_2$ catalysts with increasing Cu loading (20 wt% to 90 wt%) are shown in Fig. 1. All the catalysts exhibit characteristic peaks of CuO at 35.4° and 38.7°. The intensity of the ceria diffraction peak at 2θ = 28.4° gradually

**Table 1.** Characteristics of Cubic Cu-$Ce_{0.8}Zr_{0.2}O_2$ Catalysts

| Cu content (wt%) | Catalyst S.A. ($m^2/g$)[a] | CuO crystallite size (nm)[b] | Support crystallite size (nm)[b] | Cu dispersion (%)[c] |
|---|---|---|---|---|
| 20 | 155.7 | 16.2 | 4.0 | 7.8 |
| 40 | 136.5 | 18.1 | 3.0 | 7.3 |
| 60 | 114.6 | 19.2 | 3.4 | 6.9 |
| 80 | 86.2 | 21.9 | 3.6 | 5.6 |
| 90 | 66.6 | 22.4 | N.A.[a] | 3.6 |

[a] Estimated from $N_2$ adsorption at -196°C
[b] Estimated from XRD
[c] Estimated from $N_2O$-chemisorption

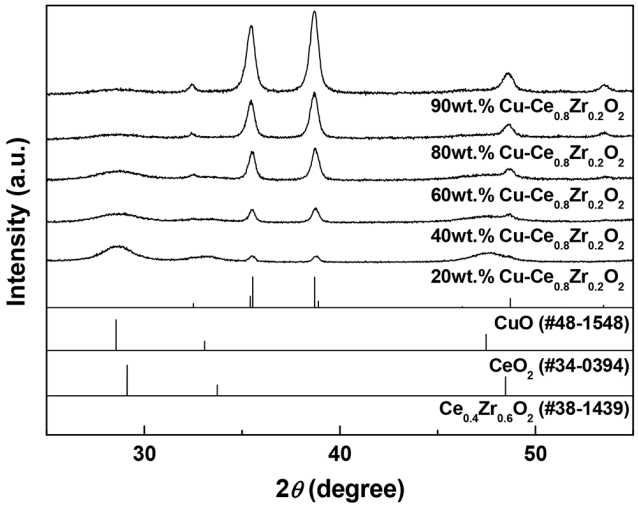


**Fig. 1.** XRD patterns of Cu-$Ce_{0.8}Zr_{0.2}O_2$ catalysts with Cu loading from 20 to 90 wt%.

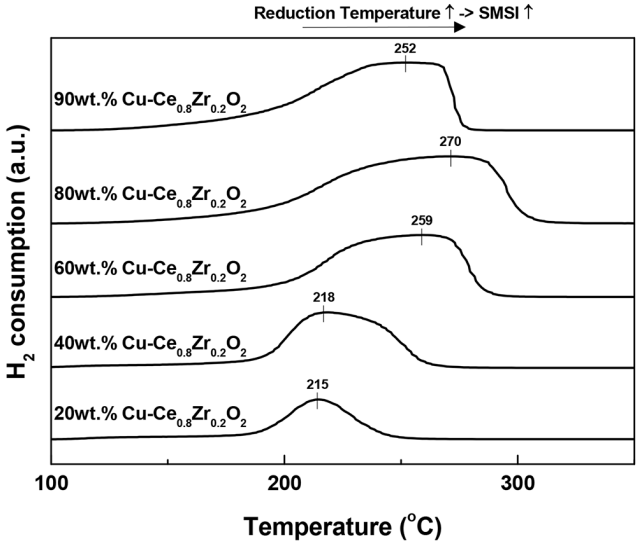


**Fig. 2.** TPR patterns of Cu-$Ce_{0.8}Zr_{0.2}O_2$ catalysts with Cu loading from 20 to 90 wt%.

decreases with increasing Cu content, indicating a decreasing degree of crystallinity. The average CuO crystallite sizes in the *x* wt% Cu-$Ce_{0.8}Zr_{0.2}O_2$ catalysts were calculated according to the Scherrer equation and are listed in Table 1. The average CuO crystallite size decreases with decreasing Cu loading. The results indicate that Cu is dispersed on the surface of cubic $Ce_{0.8}Zr_{0.2}O_2$ upon forming small crystals of CuO. Similar results have been reported by Li et al. [14].

The TPR profiles of the catalysts are presented in Fig. 2. All the catalysts exhibit a broad reduction peak attributed to the combined reduction of highly dispersed CuO (at lower temperature) and CuO associated to ceria (at higher temperature). The higher temperature shoulder peak shifts to a higher value and simultaneously becomes broader with increasing Cu loading up to 80 wt%. However, it shifts back to a lower temperature in the case of the 90 wt% Cu-$Ce_{0.8}Zr_{0.2}O_2$ catalyst. The shift of the shoulder peak toward higher temperature indicates an increasing interaction between CuO and cubic $Ce_{0.8}Zr_{0.2}O_2$ support, which diminishes beyond 80 wt% Cu loading. This may be due to the separation of CuO from the catalyst at Cu loadings beyond 80 wt%. A strong interaction between CuO and catalyst material has been reported to result in stable catalytic performance [5].

The BET surface areas of the catalysts are presented in Table 1. The BET surface areas decrease with increasing Cu loading. The Cu dispersions in the catalysts were measured using $N_2O$-chemisorption, revealing that the dispersion of Cu decreases with increasing Cu loading. The values for Cu dispersion range from 3.6% to 7.8%, with the 20 wt% Cu-$Ce_{0.8}Zr_{0.2}O_2$ catalyst exhibiting the highest value (7.8%). This indicates that the 20 wt% Cu-$Ce_{0.8}Zr_{0.2}O_2$ catalyst possesses the smallest Cu particle size among the prepared catalysts.

### 3.2. Reaction Results

Fig. 3 shows the WGS activities of the catalysts as a function of reaction temperature in the range of 240℃ - 320℃. The results clearly show that Cu loading has a strong influence on the WGS activity. The catalytic activity increases with increasing Cu loading from 20% to 80%. Further increase in Cu loading does not improve catalytic activity. The 80 wt% Cu-$Ce_{0.8}Zr_{0.2}O_2$ catalyst exhibits the highest activity among the tested catalysts over the examined temperature range. However, the 90 wt% Cu-$Ce_{0.8}Zr_{0.2}O_2$ catalyst exhibits inferior activity than those of

**Table 2.** Turnover Frequency, Cu Surface Atoms, and Activation Energy Results with Cu Loading over Cubic Cu-$Ce_{0.8}Zr_{0.2}O_2$ Catalysts

| Cu loading (wt%) | No. Cu surface atoms ($10^{20}$ atoms/$g_{cat}$) | Turnover frequency | $X_{co}$ at 210°C (%) | Ea (kJ/mol) |
|---|---|---|---|---|
| 20 | 1.48 | 0.039 | 7.8 | 34 ± 2 |
| 40 | 2.77 | 0.035 | 12.9 | 33 ± 1 |
| 60 | 3.92 | 0.033 | 17.4 | 33 ± 1 |
| 80 | 4.25 | 0.031 | 17.8 | 31 ± 1 |
| 90 | 3.07 | 0.033 | 11.4 | 33 ± 1 |

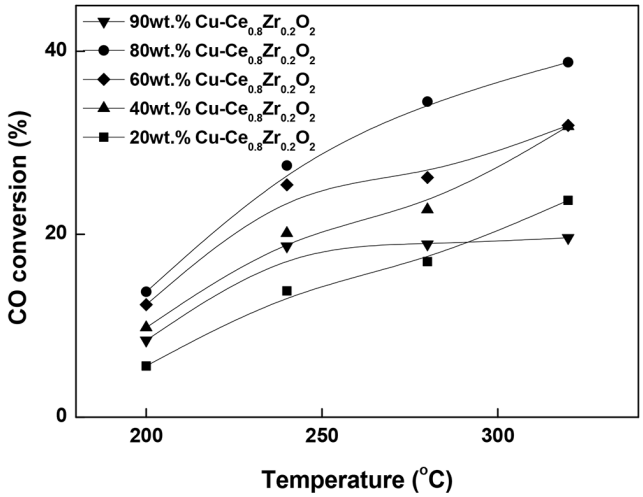


**Fig. 3.** CO conversion with reaction temperature over cubic Cu-$Ce_{0.8}Zr_{0.2}O_2$ catalysts with Cu loading from 20 to 90 wt% ($H_2O$/($CH_4$ + CO + $CO_2$) = 2.0; GHSV = 150,494 $h^{-1}$).

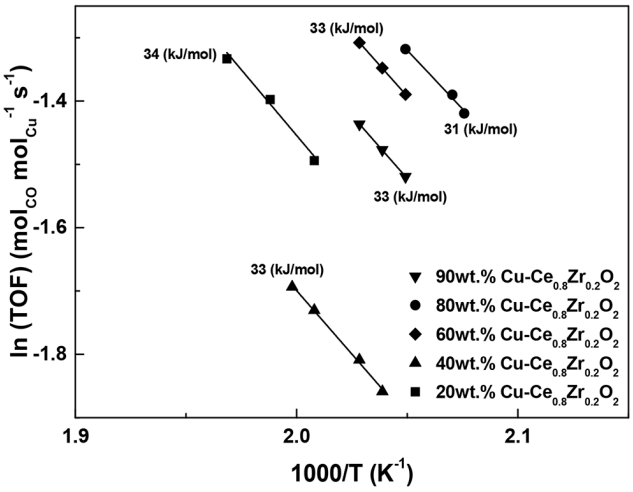


**Fig. 4.** Arrhenius plots of turnover frequency of CO conversion obtained over cubic Cu-$Ce_{0.8}Zr_{0.2}O_2$ catalysts with Cu loading from 20 to 90 wt% ($H_2O$/($CH_4$ + CO + $CO_2$) = 2.0; GHSV = 150,494 $h^{-1}$).

the 40 wt%, 60 wt%, and 80 wt% Cu-$Ce_{0.8}Zr_{0.2}O_2$ catalysts but superior activity compared with the 20 wt% Cu-$Ce_{0.8}Zr_{0.2}O_2$ catalyst. Thus, a Cu loading of 80 wt% is optimal for the LTS reaction. The activity results indicate that the catalytic performance in this study does not depend on either surface area or metal dispersion. However, it depends on the extent of interaction between CuO and the support. Thus, the excellent activity of the 80 wt% Cu-$Ce_{0.8}Zr_{0.2}O_2$ catalyst is primarily because of the strong interaction between the supported CuO and the $Ce_{0.8}Zr_{0.2}O_2$ oxide.

TOF, surface Cu atoms, and activation energy results are summarized in Table 2. The number of surface Cu atoms was calculated from the Cu dispersion and Cu loading data. The number of surface Cu atoms increases with increasing Cu loading from 20% to 80%. However, further increase in Cu loading beyond 80 wt% decreases the number of surface Cu atoms, typically due to sintering by excess Cu. This result is consistent with the CO conversion and TPR results. We can conclude that the number of surface Cu atoms on the catalyst support strongly affects the catalytic performance. Thus, the high catalytic activity of the 80 wt% Cu-$Ce_{0.8}Zr_{0.2}O_2$ catalyst is primarily attributed to the interaction between CuO and $Ce_{0.8}Zr_{0.2}O_2$, which results from the abundant surface Cu atoms. The TOF results were calculated from separate kinetic measurements that were obtained under differential GHSV (150,494 $h^{-1}$), considering the results of the $N_2O$-chemisorption experiments. 20 wt% Cu-$Ce_{0.8}Zr_{0.2}O_2$ catalyst shows the highest TOF among the tested catalysts because of the highest Cu dispersion. In fact, the trend of TOFs is similar to that of Cu dispersion.

The TOF results are summarized in the Arrhenius-type diagram in Fig. 4, where the TOFs obtained from the examined catalysts are plotted as a function of the reaction temperature. The activation energies ($E_a$) of the WGS reactions over the Cu-$Ce_{0.8}Zr_{0.2}O_2$ catalysts were calculated from the slopes of the fitted lines in Fig. 4 and are summarized in Table 2. The activation energies range from 31 ± 1 to 34 ± 2 kJ $mol^{-1}$, with the 80 wt% Cu-$Ce_{0.8}Zr_{0.2}O_2$ catalyst exhibiting the lowest activation energy of 31 ± 1 kJ $mol^{-1}$. Notably, the highest CO conversion over the Cu-$Ce_{0.8}Zr_{0.2}O_2$ catalysts corresponds to the lowest activation energy. Thus, we can reason that the role of Cu is to lower the barrier for oxygen transfer from the support to the metal, thereby facilitating the oxidation of adsorbed CO.

Fig. 5 shows the product selectivity for $CO_2$ and $CH_4$ of the reactions over Cu-$Ce_{0.8}Zr_{0.2}O_2$ catalysts with different Cu loadings. Almost 100% $CO_2$ selectivity is achieved with all the prepared catalysts, indicating that the amount of Cu on the cubic $Ce_{0.8}Zr_{0.2}O_2$ catalyst does not influence product selectivity for the LTS reaction.

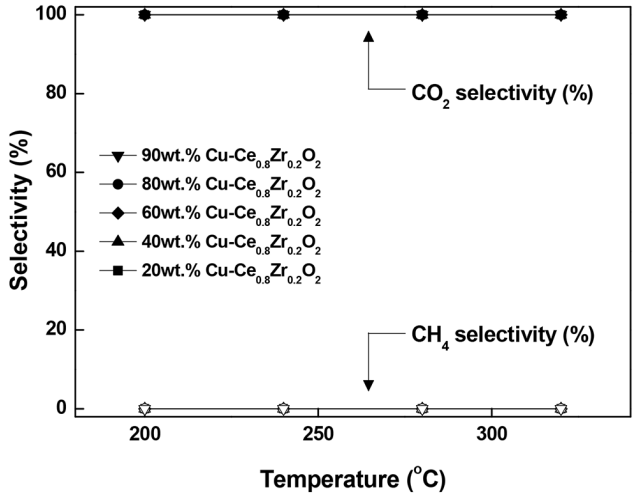


**Fig. 5.** Selectivity to $CO_2$ and $CH_4$ with reaction temperature over cubic Cu-$Ce_{0.8}Zr_{0.2}O_2$ catalysts with Cu loading from 20 to 90 wt% ($H_2O/(CH_4 + CO + CO_2)$ = 2.0; GHSV = 150,494 $h^{-1}$).

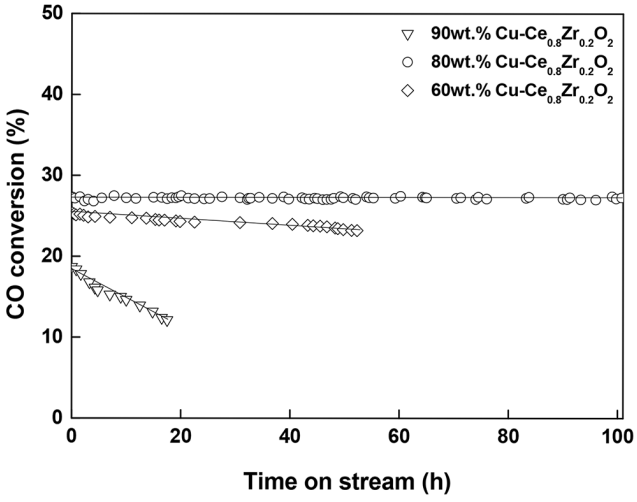


**Fig. 6.** Time on stream data over cubic Cu-$Ce_{0.8}Zr_{0.2}O_2$ catalyst with the Cu loading of 60, 80, and 90 wt% ($H_2O/(CH_4 + CO + CO_2)$ = 2.0; GHSV = 150,494 $h^{-1}$, $T$ = 240°C, TOS = 100 h).

The durability of a WGS catalyst is very important for its industrial application. Therefore, to assess the stability of the optimized catalyst (80 wt% Cu-$Ce_{0.8}Zr_{0.2}O_2$), a long-term WGS reaction test was performed at 270°C and at a high GHSV of 150,494 $h^{-1}$ for 100 h (Fig. 6). Interestingly, the 80 wt% Cu-$Ce_{0.8}Zr_{0.2}O_2$ catalyst exhibits considerably stable catalytic performance, and detectable deactivation of the catalyst was not observed ($X_{CO}$ > 27% at 270°C for 50 h). Thus, the 80 wt% Cu-$Ce_{0.8}Zr_{0.2}O_2$ catalyst exhibits both highest WGS activity and stable CO conversion, which is attributed to the strong interaction between CuO and the support. This result clearly demonstrates that 80 wt% Cu is the optimum loading for the $Ce_{0.8}Zr_{0.2}O_2$ support both in terms of activity and stability.

The excellent catalytic performance of the Cu-$Ce_{0.8}Zr_{0.2}O_2$ catalyst can be explained as follows: First, the number of surface Cu atoms is an important factor for the WGS reaction. $N_2O$-dispersion results show that the number of surface Cu atoms in the 80 wt% Cu-$Ce_{0.8}Zr_{0.2}O_2$ catalyst is the highest among the prepared catalysts. The abundance of surface Cu atoms in the catalyst is an important factor for metal dispersion and the stability against sintering of the Cu nanoparticles on the support. Furthermore, an increase in the number of surface Cu atoms helps to improve oxygen mobility at the surface of the support. As a result, the 80 wt% Cu-$Ce_{0.8}Zr_{0.2}O_2$ catalyst exhibits the highest surface Cu atoms and the lowest activation energy in the single-stage WGS reaction.

In addition, this excellent catalytic performance ($X_{CO}$ and stability) can be explained with the reduction patterns obtained by TPR. The 80 wt% Cu-$Ce_{0.8}Zr_{0.2}O_2$ catalyst reduces at 270°C, which is the highest reduction temperature observed in the TPR profiles of the investigated catalysts. The strong interaction between CuO and $Ce_{0.8}Zr_{0.2}O_2$ catalyst is probably responsible for this catalyst exhibiting the highest thermal stability among the prepared catalysts. As a result, the 80 wt% Cu-$Ce_{0.8}Zr_{0.2}O_2$ catalyst exhibits high activity with good stability, even at the extremely high GHSV of 150,494 $h^{-1}$.

## 4. Conclusions

Among the catalysts prepared in this study, the 80 wt% Cu-$Ce_{0.8}Zr_{0.2}O_2$ catalyst exhibits the highest CO conversion in the temperature range from 200°C to 400°C at a GHSV of 150,494 $h^{-1}$. In addition, it exhibits stable activity at 240°C for 100 h. The excellent catalytic performance of this catalyst is primarily because of the high abundance of surface Cu atoms and the low activation energy, which result from the strong interaction between CuO and $Ce_{0.8}Zr_{0.2}O_2$ support. As a result, the 80 wt% Cu-$Ce_{0.8}Zr_{0.2}O_2$ catalyst exhibits stronger resistance against Cu sintering. Therefore, 80 wt% is the optimal Cu loading for the co-precipitated Cu-$Ce_{0.8}Zr_{0.2}O_2$ catalysts for the low-temperature WGS reaction.

## Acknowledgments

This research was supported by Basic Science Research Program through the National Research Foundation of Korea (NRF) funded by the Ministry of Science, ICT & Future Planning (2016R 1C1B1015829).

This article was presented at the 2017 International Environmental Engineering Conference (IEEC2017) held on 15-17 November 2017, Jeju, Korea.

## References

1. Azzam KG, Babich IV, Seshan K, Lefferts L. Bifunctional catalysts for single-stage water-gas shift reaction in fuel cell applications. Part 1. Effect of the support on the reaction sequence. *J. Catal.* 2007;251:153-162.

2. Jha A, Jeong DW, Lee YL, et al. Chromium free high temperature water-gas shift catalyst for the production of hydrogen from waste derived synthesis gas. *Appl. Catal. A. Gen.* 2016;522:21-31.
3. Jha A, Jeong DW, Shim JO, et al. Hydrogen production by the water-gas shift reaction using $CuNi/Fe_2O_3$ catalyst. *Catal. Sci. Technol.* 2015;5:2752-2760.
4. Park JW, Lee SW, Lee CB, et al. Single-stage temperature-controllable water gas shift reactor with catalytic nickel plates. *J. Power Sources* 2014;247:280-285.
5. Jeong DW, Na HS, Shim JO, et al. Hydrogen production from low temperature WGS reaction on co-precipitated $Cu-CeO_2$ catalysts: An optimization of Cu loading. *Int. J. Hydrogen Energy* 2014;39:9135-9142.
6. Villar VD, Barrio L, Helmi A, et al. Effect of Re addition on the WGS activity and stability of $Pt/CeO_2-TiO_2$ catalyst for membrane reactor applications. *Catal. Today* 2016; 268:95-102.
7. Reina TR, Ivanova S, Centeno MA, Odriozola JA. Boosting the activity of a $Au/CeO_2/Al_2O_3$ catalyst for the WGS reaction. *Catal. Today* 2015;253:149-154.
8. Ammal SC, Heyden A. Origin of the unique activity of $Pt/TiO_2$ catalysts for the water-gas shift reaction. *J. Catal.* 2013;306: 78-90.
9. Aranifard S, Ammal SC, Heyden A. On the importance of metal-oxide interface sites for the water-gas shift reaction over $Pt/CeO_2$ catalysts. *J. Catal.* 2014;309:314-324.
10. Jeong DW, Na HS, Shim JO, Jang WJ, Roh HS. A crucial role for the $CeO_2-ZrO_2$ support for the low temperature water gas shift reaction over $Cu-CeO_2-ZrO_2$ catalysts. *Catal. Sci. Technol.* 2015;5:3706-3713.
11. Djinovic P, Batista J, Levec J, Pintar A. Comparison of water-gas shift reaction activity and long-term stability of nanostructured $CuO-CeO_2$ catalysts prepared by hard template and co-precipitation methods. *Appl. Catal. A. Gen.* 2009;364: 156-165.
12. Jeong DW, Subramanian V, Shim JO, et al. High-temperature water gas shift reaction over Fe/Al/Cu oxide based catalysts using simulated waste-derived synthesis gas. *Catal. Lett.* 2013;143:438-444.
13. Subramanian V, Jeong DW, Han WB, Jang WJ, Shim JO, Roh HS. $H_2$ production from high temperature shift of the simulated waste derived synthesis gas over magnetite catalysts prepared by citric acid assisted direct synthesis method. *Int. J. Hydrogen Energy* 2013;38:8699-8703.
14. Li P, Feng L, Yuan F, et al. Effect of surface copper species on NO + CO reaction over $xCuO-Ce_{0.9}Zr_{0.1}O_2$ catalysts: In situ DRIFTS studies. *Catalysts* 2016;6:124-142.